J. Synchrotron Rad. (1999). **6**, 875–890

Muscle contraction: challenges for synchrotron radiation†

Katsuzo Wakabayashi[a]* and Naoto Yagi[b]

[a]Division of Biophysical Engineering, Graduate School of Engineering Science, Osaka University, Toyonaka, Osaka 560-8531, Japan, and [b]SPring-8, Japan Synchrotron Radiation Research Institute (JASRI), Kamigori, Hyogo 678-12, Japan.
E-mail: waka@bpe.es.osaka-u.ac.jp

(*Received 8 April 1999; accepted 10 May 1999*)

The molecular mechanism of muscle contraction remains one of the major unresolved problems in biology. Muscle contraction occurs when the two sets of thin (actin) and thick (myosin) filaments slide past each other, powered by adenosine triphosphate (ATP). The central problem to be elucidated is to find out how force generation or sliding in muscle is associated with major conformational changes in the two proteins, actin and myosin, when they interact with each other. X-ray diffraction is the only technique for pursuing the structural events in the contraction process with spatial resolution (1–60 nm) and time resolution (milliseconds or less) in a living cell. Because of its inherent weak diffractor of X-rays, the use of synchrotron radiation as an intense source was inevitable for diffraction studies of muscle. Recent synchrotron X-rays have extended the diffraction pattern to atomic resolution, providing an important structural basis for the molecular mechanism underlying the whole process of muscle contraction. The analysis of the diffraction pattern has been much more sophisticated in the benefit of the determination of the atomic structures of actin and myosin. For understanding the dynamic function of proteins and their interaction in a cell at an atomic level as an ultimate goal in structural biology, muscle research has been its best example. It will continue to be a challenging field in life science. In this article the authors' own research activities in the muscle field which have been performed using synchrotron radiation are described and future challenges are discussed.

Keywords: muscle contraction; skeletal muscle; X-ray fibre diffraction; X-ray solution scattering; acto-myosin motor.

1. Introduction

Muscle cells are molecular machines that convert chemical energy into mechanical energy (force) with a high efficiency of ~60%. The molecular mechanism by which this conversion process (*i.e.* muscle contraction) occurs remains as one of the major unresolved problems in biology. Muscle contraction takes place when two proteins, actin and myosin, interact with each other, powered by hydrolysis of adenosine triphosphate (ATP). In a muscle cell each protein exists as a fibrous assembly. In the early 1950s it was shown that the two sets of filaments slide past each other without the length of both filaments changing very much (Huxley & Niedergerke, 1954; Huxley & Hanson, 1954). This proposal is fundamental to our present understanding of how a muscle operates. Since then, important questions have been raised. What makes the myosin and actin filaments slide past each other? What switches the actin–myosin motor system on and off? They have been investigated chemically and physically as well as physiologically to elucidate such mechanisms. X-ray diffraction is the only technique for pursuing the structural events with appropriate spatial resolution (1–60 nm) and time resolution (milliseconds or shorter) in a living state or intact tissue. Modern X-ray diffraction studies of muscle were pioneered by Huxley & Brown (1967) and they gave the first detailed description of muscle diffraction patterns. By that time the conventional X-ray source had reached the point of limited return, raising the need for X-rays of much higher intensity to allow two-dimensional measurements in a very short time and time-resolved experiments in a millisecond order of time resolution. This need has been answered by the development of synchrotron radiation from a storage ring which can provide a stable X-ray beam of an extremely high intensity (see Holmes & Rosenbaum, 1998). Much higher fluxes of synchrotron X-rays are now available, and novel detectors can be used, enabling us to measure the improved quality of the X-ray diffraction patterns extending to atomic resolution in various stages of muscle contraction and study dynamic structural changes on the millisecond or shorter time scale. The analysis of the X-ray diffraction pattern from a striated muscle has been much

† §§1, 2, 6 and 9 of this article were written jointly by KW and NY; §§3, 5 and 7 by KW; §§4 and 8 by NY.

more sophisticated in the benefit of the determination of the atomic structure of the constituent proteins. X-ray diffraction is the most powerful technique providing a structural basis for the mechanisms underlying the whole process of muscle contraction. The availability of new synchrotron radiation sources with extremely high brilliance will open up the possibility of producing a three-dimensional movie of the whole process of muscle contraction.

X-ray diffraction of muscle may have been regarded as a unique field in synchrotron radiation science. It is just a field of structural biology, but quite an exceptional one. Its uniqueness comes from it being more like physiology than crystallography. For those who are not familiar with muscle physiology, it may be difficult to understand why so much effort is spent on measuring a time course of intensity change. It is necessary to have enough knowledge of muscle physiology and biochemistry to find the time courses interesting. However, not only in muscle studies but also in structural biology, in general, the final goal is to elucidate the structural basis of the protein function. In this regard, muscle research is not unique at all. Indeed, the atomic structures of actin and myosin have caused considerable progress in muscle science (*e.g.* Reedy, 1993; Holmes, 1997). What makes muscle experiments unique is that X-ray diffraction experiments can be performed on a living cell because striated muscle has a highly three-dimensional order. Apart from the fact that it can be performed on living cells, X-ray diffraction experiments on muscle are not essentially different from other crystallographic experiments. What is required is to record a diffraction pattern of high quality (large number of pixels, wide dynamic range, high spatial resolution) at a high time resolution. Thus, technical developments for muscle experiments have been found useful in other experiments ranging from protein crystallography to polymer science, especially in time-resolved experiments. Earnest interest in the molecular mechanism of muscle contraction has been the driving force for the development of synchrotron radiation in life science (Huxley & Holmes, 1997; Holmes & Rosenbaum, 1998).

2. Structure and contraction of skeletal muscle

Striated muscle has a highly ordered structure with clear striations along the long axis of the muscle cell which arises from regular arrangements of the two kinds of filaments. Striated muscle contraction occurs by relative sliding between thin (actin) and thick (myosin) filaments in an interdigitating manner. The sliding or contractile force is thought to be generated by cyclic interactions of myosin heads projecting from the thick filaments with actin in the thin filaments, powered by hydrolysis of ATP. Thus, muscle contraction is a physical process that transduces the chemical energy of ATP into the mechanichal energy which produces a directional motion (shortening). It is controlled by modulation of free calcium ions within the cell. Vertebrate skeletal muscles are the principal example of a striated muscle used in muscle research and are focused in this article.

2.1. *Physiological states of muscle*

There are three basic physiological states of the muscle: resting, contraction and rigor. When the muscle cell has a high concentration of ATP ($\sim 5 \times 10^{-3}\,M$) and very low concentration of free calcium ions ($\sim 10^{-7}\,M$), the muscle is in the resting state and easily extended with no force generation. When a living muscle is stimulated electrically, calcium ions are rapidly liberated from intracellular membrane vesicles to the interior of the cells and initiate active interactions between actin and myosin, subsequently leading to shortening of the muscle, if the muscle is free to move (called isotonic contraction). If the muscle is held at constant length, this leads to the production of a force (called isometric contraction). When a muscle is brought into a state of ATP exhaustion, it assumes the state of rigor mortis, *i.e.* becomes stiff and inextensible. This rigor state is a consequence of the permanent interaction of myosin heads with actin. A similar state has been thought to exist in the hydrolysis cycle of ATP in active muscle.

2.2. *Structure of a sarcomere*

The myofibrils lie parallel to each other in a single muscle cell and each myofibril is made up of thousands of identical repeating units called a sarcomere, which is the smallest functional and structural unit of a striated muscle. In the sarcomere the thin and thick filaments lie parallel to each other (Fig. 1*a*). The thick filaments are centrally placed, with each end interdigitating with an array of thin filaments that emanate from both ends (called the Z-lines) of the sarcomere. The Z-line connects actin filaments with one polarity in one sarcomere to an array of opposite polarity in the next. The thick filaments overlap with the parts of the thin filaments in an A-band, whereas the region from the end of the A-band through the Z-line to the next A-band forms an I-band where only thin filaments are present.

The thin filament consists mainly of three proteins: actin, troponin and tropomyosin (Fig. 1*b*). The actin molecule is a globular-like protein of about 5.5 nm in diameter. When globular actin polymerizes to form filaments, this is called F-actin. F-actin is a long helical structure, in which the actin molecules are arranged in a left-handed helix with 13 actin monomers in six turns of the helix. The axial separation between the neighbouring subunits along the filament axis is $\sim$2.75 nm. The F-actin helix can be regarded either as a two-stranded structure with a half pitch of $\sim$36.5 nm (a crossover repeat of the two strands) or a single left- or right-handed genetic helix with a pitch of $\sim$5.9 or 5.1 nm. The actin filament has a structural polarity which arises originally from the actin monomer in it. Tropomyosin is a 40 nm-long rod-like molecule and binds to actin, lying end-to-end along the two grooves of the F-actin helix. At every 38.5 nm, troponin molecules consisting of three subunits

are bound to each tropomyosin molecule. The binding or release of calcium ions to or from troponin leading to changes in tropomyosin is responsible for switching on or off the interaction between myosin and actin molecules. Thus, tropomyosin and troponin are together called the regulatory proteins, and F-actin with these regulatory proteins is termed the thin filament. The thin filament is ~10 nm in diameter and 1.0 μm long (Fig. 1*b*). Atomic structures of the actin monomer (Kabsch *et al.*, 1990; see Fig. 5), the tropomyosin (Phillips *et al.*, 1986) and part of the troponin complex (Vassylyev *et al.*, 1998) are solved by X-ray crystallography.

The thick filament consists mainly of the protein myosin which is a rod-shaped 150 nm-long molecule with two globular heads at one end (Fig. 1*c*). The rod part polymerizes to form the filament backbone of ~16 nm in diameter and 1.6 μm long, from the surface of which stick out the pairs of myosin heads. Myosin rods are packed antiparallel in the central part of the filament, making the whole filament bipolar. The myosin head has a main catalytic (ATPase) domain (~10 nm in diameter) and a C-terminal α-helical domain (~8 nm long) on which two light chain molecules are wrapped. The atomic structure is shown from its X-ray crystallography (Rayment *et al.*, 1993; see Fig. 9). The arrangement of the myosin heads projecting from the filaments is followed by the backbone structure. The thick filament has a three-stranded structure: it is composed of three coaxial helices, each with nine subunits (myosin head pairs) per turn and having a subunit axial repeat of 14.3 nm and a pitch of 9 × 14.3 nm. The true crystallographic repeat of the whole filament is 42.9 nm, one-third of the pitch of each strand due to a threefold rotational structure. The thick filament in the resting state is systematically perturbed, giving rise to reflections which are forbidden from such a regular structure (*e.g.* Wakabayashi *et al.*, 1998).

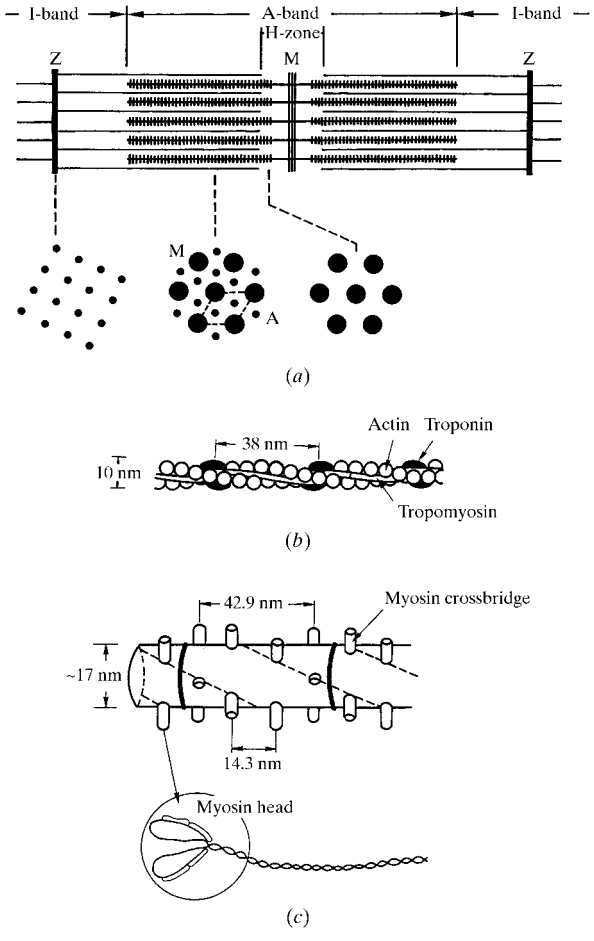

Figure 1
Schematic representation of the structure of a sarcomere in a vertebrate striated muscle. (*a*) Structure of a sarcomere. A, the thin (actin) filament and M, the thick (myosin) filament. (*b*) Fine structure of the thin filament. (*c*) Fine structure of the thick filament.

2.3. *Muscle activity*

Muscle activity is first initiated by the excitation of membranes on the muscle surface. This stimulation in turn gives rise to the release of calcium ions and these ions bind to the troponin in skeletal muscle. Subsequently, the interaction of the myosin heads with actin leads to the generation of muscle force. When intracellular calcium ions are pumped back to the vesicles, the muscle returns to a relaxing state. Thus the skeletal muscle contraction is regulated by the calcium binding to troponin.

The sliding-filament theory of muscle contraction was primarily based upon the discovery that, when a sarcomere shortens, the widths of the H-zone and I-band decrease by the same amount but the width of the A-band does not change (Fig. 2). In other words, muscle contraction occurs when the two types of filaments slide past each other, without changing their lengths very much to cause an overall shortening of the muscle. The thin filaments are the stage of acto–myosin interaction and its regulation that we are concerned with here.

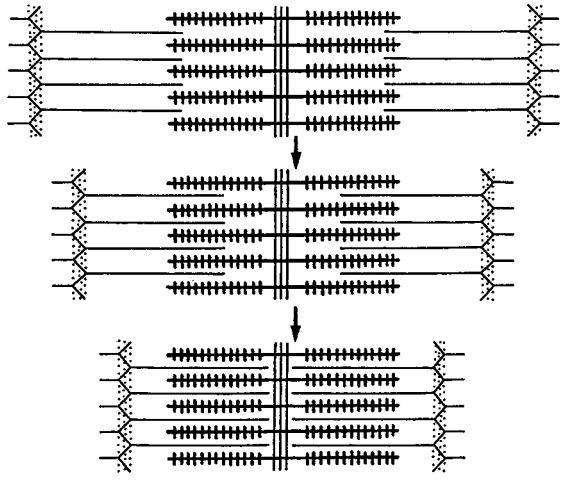

Figure 2
Shortening of the sarcomere in a striated muscle.

3. X-ray diffraction from an isometrically contracting muscle

3.1. *X-ray diffraction patterns*

The central problem to be elucidated in muscle research is to find out how force generation and movement in muscle are associated with major conformational changes in the contractile proteins, actin and myosin. X-ray diffraction is the only technique for pursuing structural events in various stages of muscle contraction. The excellent X-ray diffraction patterns from an isometrically contracting muscle were recorded first by using synchrotron X-rays and a high-sensitive and high-resolution storage phosphor area detector (Amemiya *et al.*, 1987). Fig. 3 shows the X-ray diffraction patterns from the resting (*a*), isometrically contracting (*b*) and rigor (*c*) states of a frog skeletal muscle. This type of area detector was first developed as a digital Röntgen film for medical diagnosis (see Kato *et al.*, 1985) and the unique characteristics for diffraction work were investigated (*e.g.* Amemiya *et al.*, 1988). Diffraction patterns from whole muscle are composed of the diffraction contributions from the thin (actin) and thick (myosin) filaments. Both filaments have helical structures, giving rise to two sets of layer lines with the reciprocal of the repeats

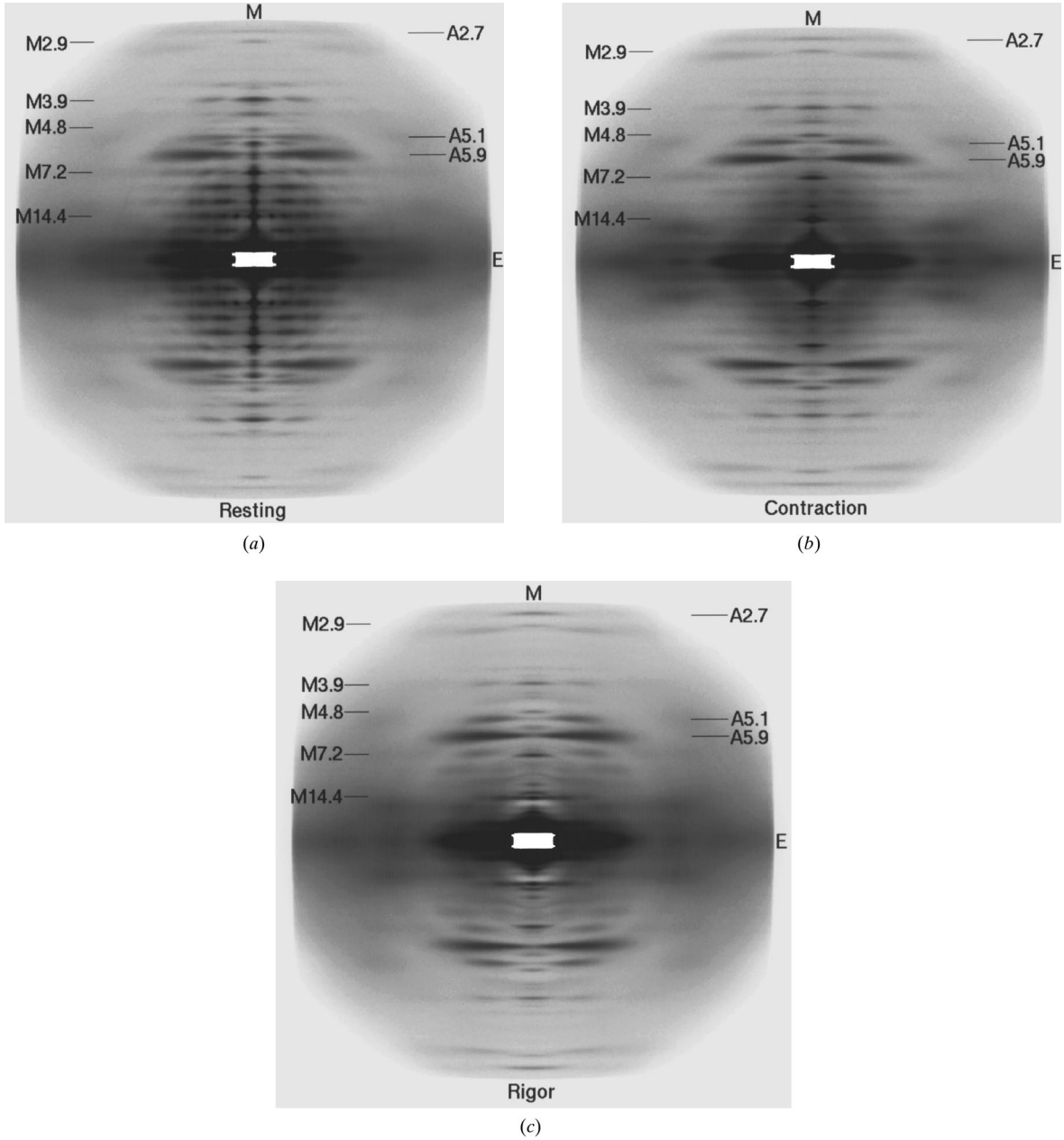

Figure 3
X-ray diffraction patterns from live frog skeletal muscles taken with an image plate. (*a*) In the resting state. (*b*) During an isometric contraction. (*c*) In the rigor state. The vertical direction is parallel to the fibre axis. M is the meridional axis and E is the equatorial axis. A2.7 is the 2.7 nm actin meridional reflection; A5.1, A5.9 are the 5.1 and 5.9 nm actin layer-line reflections, respectively. M14.4–M2.9 are the myosin-based reflections with the third (14.4), sixth (7.2), ninth (4.8), 11th (3.9) and 15th (2.9) orders of the 42.9 nm basic repeat.

of the respective filaments. Because of their different structural periodicities of both filaments, each diffraction line from the two filaments does not generally overlap. The central axis of the pattern parallel to the fibre axis is called the meridian and the central line at a right angle to the meridian is the equator. The reflections on the meridian (the meridional reflections) provide information about axial periodicities and the mass distribution along the length of the filaments. The off-meridional reflections (layer lines) represent the Fourier transform of the helical filaments, governed both by the helical parameters and by the shape of the constituent units in the filaments. Those on the equator provide information about the distribution of electron density projected onto the plane perpendicular to the fibre axis.

In a contracting state, reflecting the fact that the myosin heads move towards the neighbouring thin filaments to interact with actin, the off-meridional reflections which are arising from the helical arrangement of myosin heads around the thick filament backbone decrease in intensity markedly but do not disappear completely. On the meridian, the reflections with multiples of 14.3 nm-repeat become more prominent with ~1.3% increase in spacing (*i.e.* 14.5 nm), suggesting that the myosin heads are more perpendicularly oriented relative to the filament axis. On the other hand, most of the thin actin filament reflections become clarified with a characteristic intensification. In the rigor state, all myosin heads are known to tightly bind to the actin filaments in accordance with the helical symmetry of the actin filament (Huxley & Brown, 1967), so that most of the myosin-based layer lines disappear except on the meridian, and most of the actin-based reflections are greatly intensified with a shift in their centre of gravity towards the meridian caused by the addition of extra mass on the outer region of the thin filaments. Measurements of the intensity distributions of the layer lines show that during contraction the diffraction intensities of most of the actin-based layer lines increase without any meridional shift and also without altering their layer-line width along the equator, their amount of intensification depending on the layer lines. Unexpectedly, the first low-angle actin-based layer line inclined to decrease in intensity (Wakabayashi *et al.*, 1993). These intensity appearances are distinctly different from those in the rigor pattern. These are crucial features of the thin-filament-associated layer lines in the pattern of contracting muscle, implying that there is little sign of specific labelling by myosin heads to actin filaments as in rigor. The diffraction pattern provided strong evidence that during contraction the interaction of myosin heads with actin occurs in the incommensulate periodicities of the thin and thick filaments and possibly in an asynchronous fashion as schematically shown in Fig. 4, consistent with a view that many myosin heads go through their mechanical cycle coupled somehow to the ATPase cycle at different times on a given actin filament to produce steady force. The rigor state is actually a consequence of the permanent interaction (tight binding) of myosin heads with actin. Thus it is suggested that in an isometrically

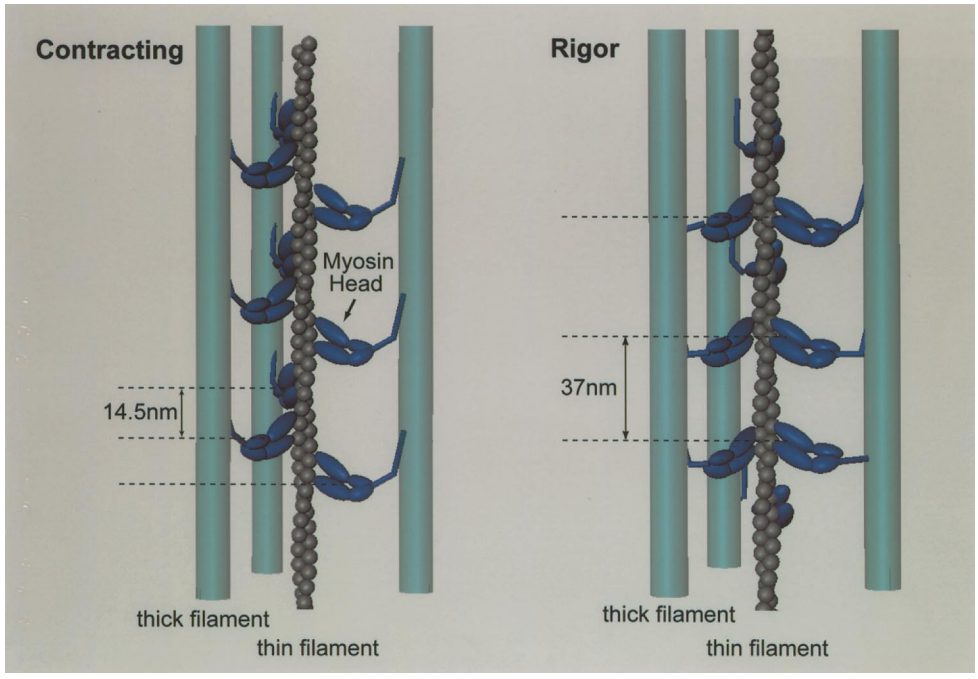

Figure 4
Schematic representation of actin–myosin interaction in the contracting state and in rigor. In the contracting state, interaction between actin and myosin occurs in an incommensurate periodicities of both filaments and the myosin heads are cycling attachment to and detachment from actin in an asynchronous fashion. In the rigor state, all myosin heads from the thick filaments are tightly and stereospecifically bound to the actin filaments in accordance with the actin helical symmetry.

contracting state there is little rigor-like stereospecific binding of the myosin heads to actin and that the actin-interacting heads are distributed through a range of configurations. Note that diffraction seeks out what is regular in a structure. Further support for this is obtained both from the lack of any intensification of the inner region of the first low-angle actin layer line, while enhanced in the rigor state, and from electron microscopic observation of quick-frozen muscle (Lenart *et al.*, 1996).

3.2. *Conformational changes of the thin actin filaments*

Using the atomic structure of the actin monomer which has been solved (Kabsch *et al.*, 1990), the F-actin filament in a frog muscle was modelled by following the procedure of Holmes *et al.* (1990), so as to obtain a reasonable fit to the observed actin-based layer-line intensities in the resting state. The data up to ~1 nm resolution have been measured and used for the analysis. In the simulation at the present resolution, the volume of each subdomain (see below) was filled with small spheres corresponding to the molecular weight. Fig. 5(*a*) is a resting model in which only tropomyosin molecules are incorporated (Ueno *et al.*, 1999). Because the complete atomic information of troponin structure is not yet available and the troponin reflections with a 38.5 nm-repeat were not included in the analysis, although troponin is, in principle, contributing to the main actin-based layer lines with a 36.5 nm repeat. The actin monomer consists of four subdomains as defined by Kabsch *et al.* (1990). These subdomains within an actin monomer in the filament are denoted by different colours in Fig. 5. The resting model is basically similar to the Holmes *et al.* (1990) model for the actin filaments reconstructed from rabbit skeletal muscle actin. Subdomains 3 and 4 lie close to the helix axis whereas subdomains 1 and 2 are outside of the filament. It is subdomain 1 that the myosin head is thought to make its strong interactions with. In the resting state, tropomyosin is in a cleft between actin subdomains 1 and 3 at the radial position of ~3.5 nm from the filament axis.

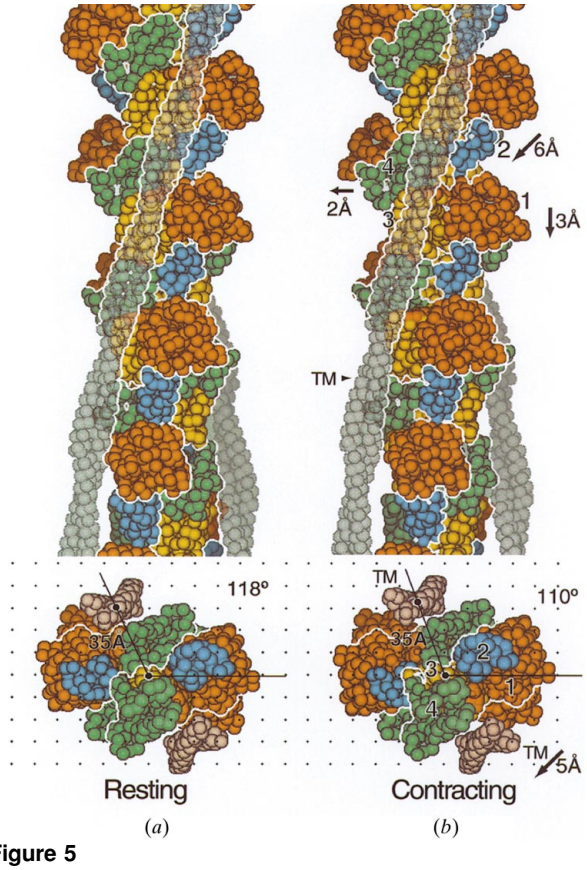

Figure 5
Modelling of the structure of thin (actin) filaments from frog skeletal muscle using the atomic data. Troponin molecules are omitted (see text). (*a*) A resting model. (*b*) A contracting model. In each, the upper is a perspective view with the pointed end upward and the lower is a cross-sectional view. The subdomains (1–4) of an actin monomer are shown in different colours. The tropomyosin molecule is indicated by TM. During contraction the direction of movement of each subdomain in actin is denoted by an arrow. The numerical values represent a magnitude of movement.

Although an interpretation of the diffraction pattern from the thin filaments in the active muscle was given above (also see Wakabayashi & Amemiya, 1991), it may not be effaced from that there are potential contributions from myosin heads interacting on actin to the thin-filament diffraction, and the cause of intensity changes of the actin-based layer lines during activation is still under investigation. Whether the observed pattern from a contracting muscle is sensitive to the structural changes within the thin filament itself or extra mass transfer from the interacting myosin heads and/or both (Maeda *et al.*, 1988) has been tested by a Fourier difference synthesis. Using the model of the actin filament plus tropomyosin in the resting state to phase the observed reflections, the slightly different set of amplitudes from the thin-filament pattern during contraction was combined with the original phases and a Fourier difference synthesis was calculated (Ueno *et al.*, 1999). Such a difference map reveals that the changes in electron density might have taken place in some places within the region of the F-actin filament, providing suggestive evidence that the intensity changes of the thin-filament-associated layer lines are caused dominantly by structural alterations of the thin filament itself rather than by the direct mass transfer associated with myosin head labelling, although structural changes of the thin filament are induced in a large part by the interaction with the myosin heads as evidenced from the very small X-ray changes during the activation of overstretched muscle in which thin and thick filaments do not overlap. The detailed results from this approach will be presented elsewhere. This appearance suggests that the thin filament and myosin heads which are arranged with a variety of configurations on the actin filaments do not diffract with strong coherency. This provided even stronger motivation for us to press for the following modelling. The observed intensity changes of the actin-based layer lines during contraction have been simulated by altering an internal structure of the thin filament (Ueno *et al.*, 1994, 1999). The results revealed that conformational

changes are made by integration of small movements of subdomains within the actin monomer and the positional change of tropomyosin strands. Fig. 5(*b*) shows the present best-fit model of the thin filament without troponin in the contracting state. In the perspective views, during contraction there was increased ruggedness of the filament surface caused by relative positional changes of each subdomain in an actin monomer. This increase in ruggedness is the main cause in the intensification of actin-based layer lines because the strength of the layer lines is determined by Fourier transform of the ruggedness (Wakabayashi & Amemiya, 1991). In the cross-sectional view seen from the M-line of the sarcomere, the fourfold rotational symmetry tends to be strengthened due to the subdomain movement within the actin monomer together with a tropomyosin shift. The reverse intensity changes in the first and second low-angle actin layer lines observed during contraction can be interpreted as this strengthening in a fourfold rotational nature. The changes in the actin domain structure during contraction are shown by arrows in Fig. 5(*b*): the largest movement occurs in subdomain 2, moving to the opposite direction of this figure by ∼0.6 nm. Subdomain 1 also moves in the opposite direction by ∼0.3 nm and slightly downward. The positions of subdomains 3 and 4 changed little, possibly contributing to define the helical structure. During contraction, tropomyosin strands shifted towards subdomains 3 and 4 by ∼8° azimuthally corresponding to ∼0.5 nm movement, but the radial distance remains almost the same as in the resting state. It has been thought that the movement of tropomyosin may be associated with a regulation mechanism: tropomyosin regulates myosin interaction with actin by altering its position on actin filament [the so-called 'steric blocking hypothesis'; see Huxley (1973)]. The present movement of tropomyosin is less than is currently thought without considering an alteration in the actin structure (also see Squire & Morris, 1998), although the possible effects of troponin molecules have been precluded in the present analysis; the mass of troponin is averaged over an actin structure with a 13/6 helical symmetry. The validity of the steric blocking model should be discussed when the structural role of troponin and its contribution are solved in the interpretation of X-ray data.

When the muscle was stretched to a half-overlap length of the thin and thick filaments in a sarcomere and stimulated, the changes in the diffraction pattern were greater than those expected from the half amount of filament overlap and showed rather similar features to those seen in the pattern from a contracting muscle with full overlap length. The structural change of thin filaments shows cooperativity in its interaction with myosin.

3.3. *Mechanical properties of the thin actin filament*

The force of the acto-myosin motor system is transmitted to the ends of the contractile unit through thin actin filaments, which have generally been thought to contribute very low compliance to the mechanochemical machinary. On this ground, the so-called 'rotating or tilting myosin crossbridge model' has been founded as the most influential molecular mechanism for muscle contraction (Huxley, 1969; Huxley & Simmons, 1971). The model postulates that the myosin heads projecting from the thick filaments attach to actin in the thin filaments (forming crossbridges with the thin filaments), pull the thin filaments towards the centre of the sarcomere and detach in a repeated cycle. The force or filament sliding might be generated by a tilting or rotating motion of the attached heads on actin. Such motion stretches the elastic component located somewhere around or within the myosin crossbridge, producing a force that displaces the thin filaments. Thus it has been assumed that the actin filament has a stiff structure on which the myosin heads can tilt or rotate. However, the assumption that both filaments are effectively stiff (inextensible) under active force generation has not been verified. Thus precise knowledge of the mechanical properties of the filaments is important for understanding the force-generation mechanism in muscle (see Goldman & Huxley, 1994).

Most recently, the mechanical properties of the thin actin filaments have been investigated in the force-generating process and by changing the force levels by imposing the length changes to an isometrically contracting muscle with X-ray diffraction techniques using synchrotron radiation (Huxley *et al.*, 1994: Wakabayashi *et al.*, 1994). The X-ray diffraction patterns were recorded using the same muscles in a two-dimensional stroboscopic technique using a rapid exchanger of the image plate (see Amemiya, 1995). For the actin-based reflections, the axial spacings of the 2.7 nm meridional reflection and of the 5.1 and 5.9 nm layer lines (see Fig. 3) were measured accurately. Within these, the

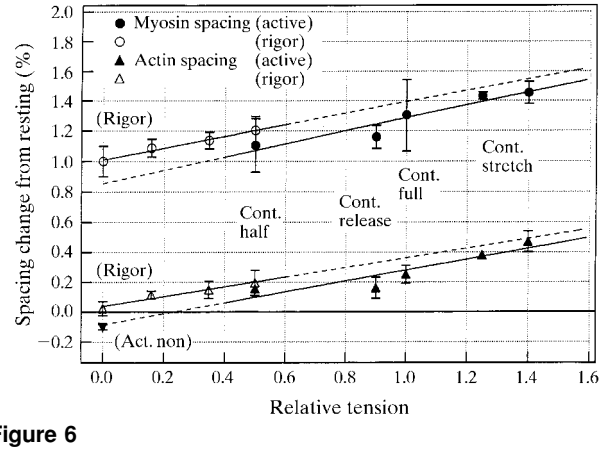

Figure 6
Spacing changes of the 2.7 nm actin-based meridional reflection and the myosin-based meridional reflections against force relative to the isometric force (P_0). Data of 'cont. half' and 'cont. full' were obtained from the experiments with contracting muscles at half- and full-filament overlap, respectively. Those of 'cont. release' and 'cont. stretch' were obtained from experiments with contracting muscles during slow length release and stretch, respectively. Data of rigor were from the rigor muscles. The data point (▼) obtained from the overstretched muscle upon activation is shown at $P_0 = 0$ for comparison. Linear regression lines were obtained by the least-squares fit to the data points.

spacing change of the 2.7 nm reflection is a direct measure of any extensibility of an actin filament. The precise measurements of small spacing changes of the much weaker 2.7 nm meridional reflection could not be made without the use of synchrotron radiation in a combination of the high-sensitive and high-resolution image plate. It was found that the peak position of the 2.7 nm reflection shifted towards the low-angle side in the transition from resting to contraction (see Fig. 3), showing an increase in the axial distance between the actin monomers. The application of stretch to a contracting muscle increased the force and increased this spacing in the same direction. Fig. 6 summarizes the spacing changes of the 2.7 nm actin meridional reflection, together with those of the myosin-based meridional reflections as the function of force relative to an isometric force (P_0) exerted by the muscle at full-filament overlap (Takezawa *et al.*, 1998, 1999). Fine linear regression lines indicate that the extensibility of the actin and myosin filaments is highly elastic. Concerning the actin filaments, the maximum increase in the spacing at the development of P_0 is ~0.36%, which was estimated from the slope. When the regression line for the actin filaments is extrapolated to zero force, the spacing change would be about −0.08%, implying that such a small amount of shortening of the filament is occurring in the early process of activation. This initial change of the actin filaments was consistent with ~0.1% spacing decrease observed when the overstretched muscle was activated by stimulation. It would be that the actin filaments could become shortened at the onset of activation and then are extended as the force develops. The net spacing change would be ~0.36% at the development of P_0. In the case of the myosin filaments, the extrapolated value of the spacing changes is ~0.86%, reporting that a large change in the myosin reflections occurs in the initial activation without force generation. Such a large change has been thought to be due to a structural rearrangement accompanying muscle activation (Huxley & Brown, 1967). About 1% spacing change was observed when the resting muscle was put into rigor without force development (see Fig. 6). In Fig. 6 there is a small but distinct difference in the spacing change between the rigor value and the extrapolated value at zero force of active data. The difference between them may correspond to ~0.1% negative change of the myosin-based meridional reflections which has also been observed upon activation of the overstretched muscle. Thus the net spacing change of the myosin filaments could be ~0.43% at P_0. The spacing changes of both filaments as the minimum values of extension (Huxley *et al.*, 1994; Wakabayashi *et al.*, 1994) indicate that the elongation of the actin filament of length 1 μm is ~3.6 nm and that of the myosin filament of length 0.8 μm per half sarcomere is ~3.4 nm under the maximum force. The results suggest that a fairly large part of the sarcomere compliance of an active muscle is caused by the compliances of the actin and myosin filaments because the total extension of the elastic elements which carries active force has been estimated to be 6–8 nm per half-sarcomere.

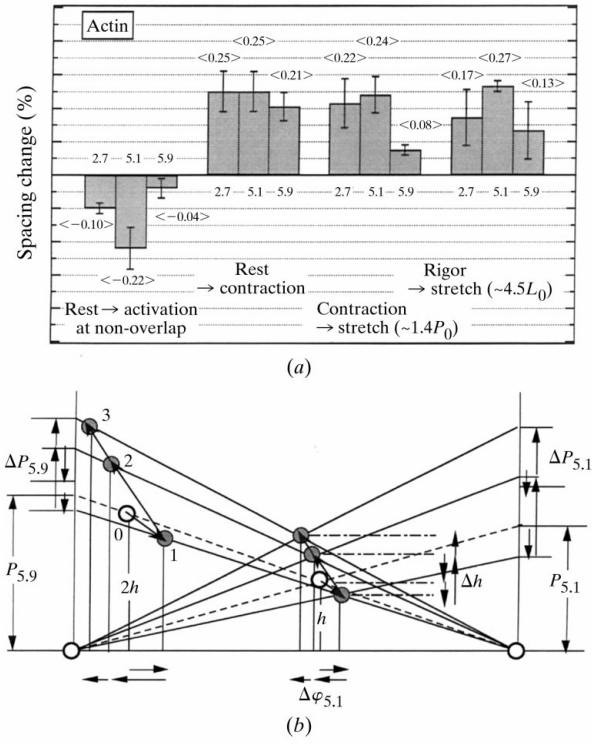

Figure 7
(*a*) Axial spacing changes of the three actin-based reflections in the transition from rest to activation at non-overlap length, rest to contraction at full overlap length, and contraction to stretching ($1.4P_0$). The last set of columns shows the data when the stretch (~4.5% of initial muscle length L_0) was imposed to the rigor muscle. (*b*) Part of the radial projection net of the actin helical structure showing the angular movement of the centre of gravity of an actin monomer unit following the filament extensibility. h, $P_{5.1}$ and $P_{5.9}$ denote the axial rise of the actin unit, the pitches of the right- and left-handed genetic helices. Δ symbols and vertical and horizontal arrows show the magnitude and direction of their changes (see text).

This finding provides important evidence that the actin filament is much more compliant than was earlier thought and necessitates a significant reconsideration of the current crossbridge model, challenging the foundation of the molecular mechanism of muscle contraction.

3.4. *Changes of the actin helical structure*

The spacing changes of the 5.1 and 5.9 nm actin-based layer lines are summarized in Fig. 7(*a*) as a histograph together with that of the 2.7 nm meridional reflection in the three transitions of muscle states: rest → initial activation, activation → contraction and contraction → stretching (Takezawa *et al.*, 1998). It is seen that in each transition the spacing changes of these three reflections are different. The differential changes are closely related to an alteration of the helical structure of an actin filament with an accompanying of the extensibility (Wakabayashi *et al.*, 1994). The centre of each monomer in the filament is projected perpendicularly from the filament axis onto the surface of a cylinderical tube which encompasses the filament and then the tube is opened out flat to obtain the radial projection

net. Fig. 7(*b*) shows an enlarged part of the whole net where the axial displacement of the actin monomers is denoted by *h*, giving rise to a 2.7 nm meridional reflection, and each angular displacement of the units in the structure is represented by an equal horizontal displacement denoted by φ, corresponding to a unit twist between axially consecutive points ($\varphi = 2\pi h/P$ where P denotes a pitch of any helix). In this net the lines of negative slope correspond to a left-handed genetic helix with a pitch of 5.9 nm ($P_{5.9}$) and those lines of positive slope to a right-handed genetic helix with a pitch of 5.1 nm ($P_{5.1}$), giving rise to the 5.9 and 5.1 nm layer lines, respectively. From the geometrical relation of this net, the following relation between changes in h and two pitches holds when their changes are small,

$$\Delta h/h = (h/P_{5.1})(\Delta P_{5.1}/P_{5.1}) + (h/P_{5.9})(\Delta P_{5.9}/P_{5.9}).$$

For the angular changes, for example from $\varphi_{5.1} = 2\pi h/P_{5.1}$, a change of the right-handed unit twist is given,

$$\Delta\varphi_{5.1} = 360^\circ \times (h/P_{5.1})(\Delta h/h - \Delta P_{5.1}/P_{5.1}).$$

If the fractional change in h reflecting directly the extensibility of the filament is different from those in the helical pitches, then the filament extensibility is accompanied by the twisting change of its helical structure. In all three cases the differential spacing changes satisfied the first relation. Thus the twisting change is associated with the extensibility of the actin filament. From the second equation, ~0.1% shortening accompanies a positive change in the twisting change ($\varphi_{5.1}$) of ~0.2° in the transition from the rest to initial activation (denoted by 0 → 1 in Fig. 7*b*). In the subsequent transition to isometric contraction (1 → 2), the net twist of the actin helical structure amounts to ~0.2°. When a stretch of ~4% initial muscle length was imposed to an isometrically contracting muscle (2 → 3), the force increases to ~1.4P_0 and the filament extension of ~0.2% with the negative change of ~0.1° in $\varphi_{5.1}$ occurs over the isometric value. Scaled to a 100% force increment, ~0.4% relative change in h would be accompanied by −0.23° in $\varphi_{5.1}$. As shown by arrows in Fig. 7(*b*), these changes indicate that the actin monomer first moves in the direction (0→ 1) in the net upon initial activation. As the force generates, it moves in the opposite direction (1→ 2) and during the stretch it further moves in almost the same direction (2→ 3). Thus the extension of the actin filaments upon the development of force always accompanies an untwisting of the right-handed genetic helix, causing ~70° anticlockwise rotation of the free end of the actin filament at P_0. The helical symmetry of the actin filament does change when the force is generated, although the change at P_0 is not as large as an alteration of the helical symmetry from 13 subunits/6 turns to 28 subunits/13 turns (Takezawa *et al.*, 1999). Upon initial activation, the right-handed genetic helix would twist slightly. Twisting motions of the actin filament would relate to the mechanics of the intermolecular contacts in a filament.

It is well known that the intensity changes of most of the thin actin-based reflections precede the development of force. Apart from the initial changes associated with the regulation mechanism, the implication is that the myosin–actin interaction is a two-step reaction which requires a non-force-generating state before production of force. The most recent studies by Huxley *et al.* (1998) revealed that the time course of the spacing changes of these actin-based reflections run closely in parallel to force development, and the changes quickly returned to zero when the force dropped to zero in response to a rapid length change applied to a contracting muscle (Huxley *et al.*, 1994). The extensibility and twisting changes of the actin filaments are closely related to the generation of force.

It is becoming clear that significant structural changes are taking place in the thin actin filament involved in its regulation and force development.

4. X-ray diffraction from a shortening muscle

Shortening is also a very important physiological function of muscles. It is caused by thick and thin filaments sliding past each other in each sarcomere. What causes them to slide has been a matter of highest interest in muscle physiology in the last 40 years. When a contracting muscle is released with an afterload, it pulls the load with a constant speed. This suggests that a certain kind of steady state is established quickly in the muscle. Because muscle shortening is a brief event, lasting only a few tens of milliseconds, synchrotron radiation is quite useful for studying the molecular structure of muscle during shortening. Early studies made by using a laboratory X-ray source were focused only on the strong equatorial reflections (Podolsky *et al.*, 1976). The results seemed to suggest that many of the myosin heads still stay close to the thin filaments even in a fast shortening. However, later studies using synchrotron radiation gave clearer views on the molecular structure in a shortening muscle (Yagi *et al.*, 1993; Yagi & Takemori, 1995; Griffith *et al.*, 1993; Piazzesi *et al.*, 1999). The detectors, such as linear and area gas detectors, an image-plate exchanger and an X-ray image intensifier, were used to record intensity changes of both myosin and actin-based reflections. Fig. 8 shows a comparison of X-ray diffraction patterns taken between an isometric contraction before shortening and during shortening near the maximum velocity using an image-plate exchanger (Yagi *et al.*, 1993). The intensities of the myosin-based meridional reflections with a 14.5 nm-repeat and those of the 5.9 and 5.1 nm actin-based layer lines decreased and that of the second myosin meridional reflection increased relative to their isometric values during shortening. The intensity decrease of the myosin meridional reflections implies that during shortening the myosin heads are on average more inclined with respect to the the filament axis than during isometric contraction: the axial orientation of the myosin heads can be different during isometric and isotonic contraction. The results indicate that even the heads located close to the thin filaments are not making such an interaction that is essential for force

production. This is evident from the intensity of actin-based layer lines which drops as the shortening speed increases. The spacing of the 14.5 nm reflection was reduced to 0.47% but still above the resting value and the 2.7 nm actin meridional reflection returned almost to the resting value. Note that the intensity distributions along the 5.1 and 5.9 nm actin layer lines were very similar in the resting state and during isometric contraction, as mentioned above, and they did not change significantly during shortening. The implication is also that the myosin–actin interaction is a two-step reaction. In a rapidly shortening muscle, although myosin heads and actin can make a collision-based first contact, they cannot enter the next step before the interaction is broken by the filament sliding. Further detailed investigation on shortening muscle will still be an interesting subject.

5. Conformational changes of the myosin heads forming various intermediates in ATP hydrolysis

It is important to clarify how the conformational changes of the myosin head relate to the energy-transducing mechanism. Conformational changes of isolated myosin heads (subfragment 1, S1) in the presence of ATP have been investigated by X-ray solution scattering using synchrotron radiation (Wakabayashi *et al.*, 1992) (Fig. 9*a*). It was first demonstrated that the radius of gyration and the maximum chord length of S1 which are estimated from the slope of the Guinier plot and the Fourier transformation of the scattering intensities decreased by ~0.3 nm and 1 nm, respectively. The results indicated that the shape of S1 became compact during hydrolysis of ATP. Analysis using the atomic structure of S1 (Rayment *et al.*, 1993) revealed a global change which pivots between the proximal domain and the long tail domain which was determined mainly by two orthogonal components of movement, making as a whole some 5 nm spinning of the distal end of the molecule (Sugimoto *et al.*, 1995, 1999) (Fig. 9*b*). The existence of two such main modes in S1 has been shown by molecular dynamic simulation, determining the molecular shape of S1 (Higo *et al.*, 1999). The experiments with several ADP + phosphate analogs mimicking various intermediates of the S1 ATPase cycle suggested that this global change of S1 occurs in the state where the hydrolysis products [ADP and phosphate, Pi (PO_4^-)] of ATP remain bound to the head, and those with ATPγS and ADP suggested that the global conformation changes little just after the initial binding of ATP and returns to the original structure in two steps, on release of phosphate and release of ADP (Wakabayashi *et al.*, 1992; Sugimoto *et al.*, 1995, 1999). These implications are consistent with the biochemical studies of the myosin ATPase reaction, although it must be directly confirmed by the time-resolved X-ray solution scattering using more intense synchrotron radiation during an S1 ATPase reaction. These results show that interaction with ATP is accompanied by substantial changes in the myosin head shape that are correlated with the key intermediate state (an S1.ADP.Pi state) of the myosin ATPase cycle. However, in an acto-myosin motor system, the myosin head creates force production only when it interacts with actin. The myosin ATPase is accelerated by actin. The conformation of the myosin head should be defined by the mechanical

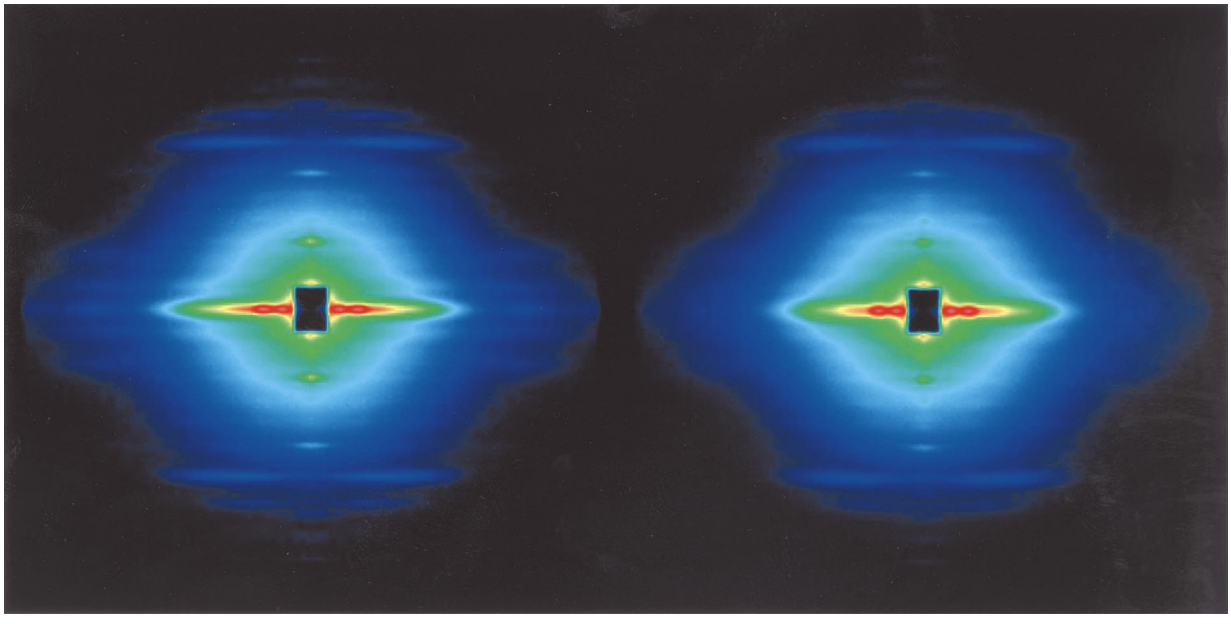

(*a*) (*b*)

Figure 8
Comparison of X-ray diffraction patterns taken between an isometric contraction before shortening (*a*) and during shortening near the maximum velocity (*b*). The patterns were recorded by using the rapid image-plate exchanger. The fibre axis is vertical. Note the intensity decreases in the meridional reflections with a 14.5 nm repeat and the 5.1 and 5.9 nm actin layer lines during shortening.

state as well as the chemical state in which it is put. Thus how such conformational changes actually correlate with force production must be shown up in an actomyosin motor system (see below).

6. Conformational changes of the myosin heads in the active muscle

Experiments have been attempted to examine whether these changes of the myosin head observed in solution are actually occurring in active muscle and how a conformational change of myosin crossbridges is related to the force generation. In our attempt a sinusoidal length perturbation at 0.5 kHz with an amplitude of 0.3% muscle length was applied to contracting muscle fibres during the plateau phase of the force development by Ca^{2+}-activation (Yagi *et al.*, 1996). This technique is one of the perturbation-response methods investigating a dynamic steady state of the system, making myosin heads interacting with actin synchronize partially and momentally by imposing small but rapid changes of muscle length to contracting muscle fibres. The relation between the force response and the intensity change of the myosin-based 14.5 nm meridional reflection (see Fig. 3) was investigated by time-resolved X-ray diffraction (in a streak mode) in a 0.2 ms time resolution using a rotating-drum image-plate system (see Amemiya, 1995). This type of experiment provides an interesting challenge to obtain direct insight into the molecular mechanism of force production (see below). The force oscillated below the isometric level in parallel to a length oscillation without any phase lag. The results are shown in Fig. 10(*a*). The force changed in phase with the length changes imposed to a contracting muscle and the intensity of the myosin reflection changed in antiphase with a change in force, indicating that there exists some coupling between the force production and structural changes occurring in the myosin during its interaction with actin. These intensity changes occur in the opposite direction to those in rigor muscle. Fig. 10(*b*) depicts a straightforward model explaining the intensity changes as the conformational changes of the myosin heads interacting with actin in response to the oscillatory length perturbation. If the structural changes of myosin are confined to its elongated tail domain of a crossbridge which is orientated more perpendicular to the filament axis in an isometrically contracting muscle, that domain displaces in the axial direction (towards the M-line of the sarcomere) in the stretching phase, resulting in a smearing out of the sharp concentrations of density at 14.5 nm intervals. In that case the motion of the heads seems to be also elastic. Together with the quick step-length-change experiments (see Piazzesi & Lombardi, 1995) (see below), this experiment provides an important result showing that structural changes are taking place in the myosin as the thin and thick filaments slide past each other, and those changes in the X-ray solution experiments may correlate with force production in active muscle. However, it should be premature to take this literally until the diffraction pattern is fully understood because many other factors contribute to the meridional reflections with a 14.5 nm repeat.

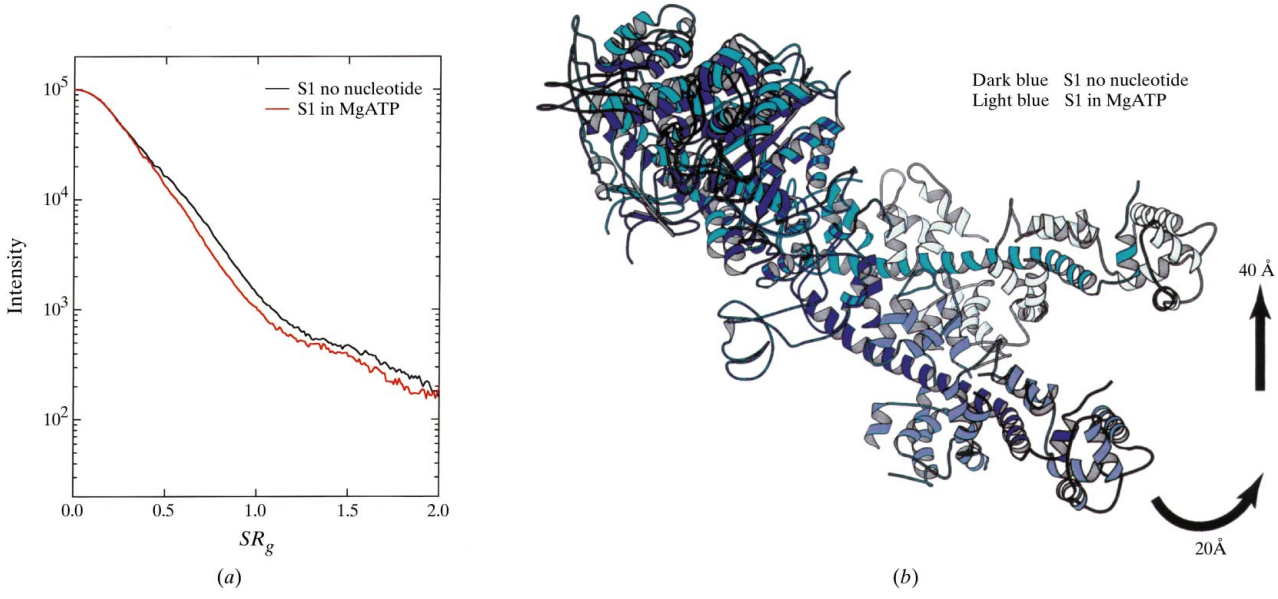

Figure 9
Conformational change of the myosin heads (subfragment-1, S1) in the presence of ATP. (*a*) The comparison of the X-ray solution scattering curves taken from S1 samples with no nucleotide and in the presence of MgATP. In this plot the deviation of the scattering curve of S1 in ATP solution from that with no nucleotide beyond $SR_g = 0.4$ (where R_g is the radius of gyration of S1) shows the distinct shape change during hydrolysis of ATP. (*b*) Modelling of the conformational change of S1 in the presence of ATP by using the atomic data of S1. When the two models are coincided with their N-terminus of the proximal domain (the catalytic domain), the distal tip of the molecule moves as shown by the arrows (vertically and azimuthally). In this figure the imaginary actin filament axis is aligned vertically in the left-hand side of the models.

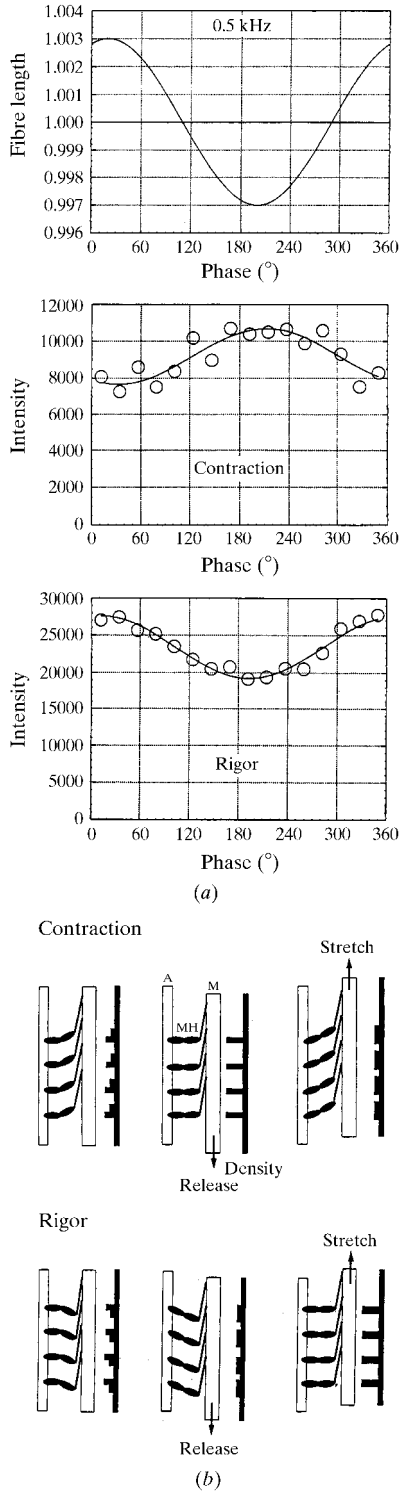

Figure 10
(*a*) Oscillatory length changes of the muscle fibres and intensity changes of the 14.5 nm myosin-based meridional reflection in one cycle. The small fibre bundle was oscillated at the frequency of 0.5 kHz and with a peak-to-peak amplitude of 0.6% of the fibre length. Top: an oscillatory length change. Middle: a change of the 14.5 nm intensity in the active state. Bottom: a change of the 14.5 nm intensity in rigor for comparison. (*b*) A straightforward model explaining the intensity changes as the motion of the myosin heads during the oscillatory length changes. Each figure in the right-hand side represents schematically the mass density of the myosin heads projected onto the fibre axis.

7. Partnership of actin–myosin as a molecular motor

In Fig. 11 we briefly summarize the conformational changes of the actin and myosin heads during contraction of skeletal muscle which have been derived from our current X-ray diffraction studies. In active muscle the myosin heads having ADP and phosphate interact first weakly with actin. In this process the structure of the actin filaments is altered as evidenced from the time-resolved intensity changes of most of the actin-based reflections which precede the development of force. As the force develops, the actin filaments could be elongated maximally by ~4 nm at its end in the coordination of conformational changes of the attached heads on release of phosphate ions and then ADP. It may be possible that a cranking action in a myosin head could be combined with the lever-arm action (corresponding to some 4 nm axial movement at its distal end),

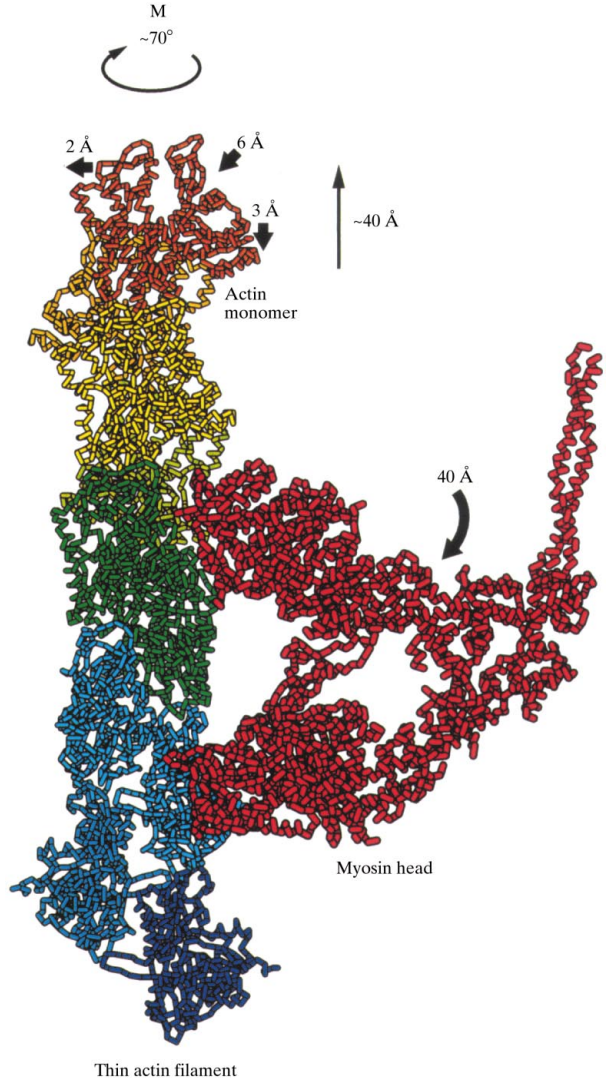

Figure 11
A scheme for coupling of force generation with specific conformational change occurring in actin and myosin. M denotes the side of the M-line in a sarcomere (the pointed end of the actin filament, upward).

imposing the torque to unscrew the actin filaments by ~70° at its end in a sarcomere. In other words the hydrolysis energy of ATP stored in the myosin head as conformational energy is transferred to the actin filament and stored as elastic energy. Their stored energy in both would be utilized as contractile force. Our X-ray diffraction studies provide evidence that coupling between these structural changes of a myosin head and actin may be directly associated with an energy-transducing mechanism in the elementary force-generating process. It is becoming clear that significant structural changes are taking place in the thin actin filament involved in its regulation and force development and that the actin filaments play a much more active role than simply rigid force transmitters in the force-generation process. Several important findings described above stimulate the foundation of a sophisticated model in a combination of peculiar structural changes of actin and myosin heads. The two proteins, actin and myosin, are equally important in the activity of force generation and sliding movement in muscle.

8. Future challenges for synchrotron radiation

8.1. *Experimental challenges*

8.1.1. *Use of a parallel beam*. The extremely parallel beam from an insertion device equipped in a low-emittance storage ring yields a diffraction pattern with an unusually good angular resolution and a high signal-to-noise ratio. In this way, low-angle X-ray patterns extending into reciprocal spacings of the sarcomere repeat can be recorded with very high angular separation in a very short time. Fig. 12 shows an example of a high-resolution X-ray diffraction pattern of live frog muscle which was taken using an undulator beam at the Tristan main ring at KEK (Yagi *et al.*, 1996; Wakabayashi *et al.*, 1998). The vertical divergence angle of the first harmonic of the undulator was ~10 μrad at 8 GeV operation. The well collimated beam made it possible to resolve, with a high-angular resolution of ~700 nm, the closely spaced diffraction peaks on the meridian which arise from the sampling of the sarcomere structure (mainly from interference between the two halves of the thick filaments centred on the M-line in a sarcomere). The pattern had an extremely high signal-to-noise ratio.

8.1.2. *Mechanical transients*. When an isometrically contracting muscle fibre is released in a stepwise manner in a very short time (<1 ms), the force drops with the length and then undergoes a characteristic recovery to the isometric level (Huxley & Simmons, 1971). The drop in force shows that there is an elastic component in the fibre, which may be in myosin heads or in the thin and thick filaments or in both as discussed above. According to Huxley & Simmons (1971), the recovery phase is made of three phases: quick recovery of force (phase 2), a short plateau or even a slight decrease in force (phase 3), and a final return to the isometric level (phase 4). Phase 2 has been postulated as an isomerization of the actin–myosin complex, that is due to conformational changes of a bound head without detachment or reattachment. The structural changes associated with this transient change in force have been studied using a single muscle fibre (see Piazzesi & Lombardi, 1995). The intensity change in the 14.5 nm meridional reflection was extensively examined with a higher time resolution (~0.1 ms) and the results might be consistent with the myosin head changing axial conformation to redevelop force. As mentioned above, for a full account for this transient change in force, the experiments must be extended to other myosin reflections including the weaker actin reflections.

In the transient changes in force, the measurements of spacing changes of the thin and thick filaments at a higher time resolution will be an important example of future experiments using synchrotron radiation. Although the filament length has been shown to change proportionally with force, it has not been sufficiently shown that the spacing changes take place simultaneously with a change in force. This is an important point because the force recovery after a quick length change (force transients described above) takes place in 1 ms. It is possible that other structural changes which affect the axial dimension or arrangement of myosin and actin molecules are also taking place. Thus, it still remains to be decided whether the filaments behave purely elastically to a change in force. In order to examine if the filaments are really elastic or not, we have to measure the time course of the spacing changes during and after a quick length change of muscle. To avoid complication caused by the rapid force recovery, the length change must be performed within 1 ms and thus the time resolution of X-ray measurement should be 0.1 ms. This type of experiment may be performed on a whole muscle (with several mm in width) (*e.g.* Huxley *et al.*, 1994) but, for precise force control, a single fibre (50–100 μm in width) is preferred. For this purpose, what is truly required is not the flux but the flux density (the brightness) with a beam size of 0.1 mm by a few mm.

It may be more effective to use sinusoidal length changes with variable frequencies than the use of step length changes. At low amplitude of oscillation it is expected that myosin crossbridge might be partially synchronized so that one should be able to record diffraction patterns from various parts of the cycle. Such an experiment with a bundle of fibres has been described above. The experiment with higher frequency was attempted using a single fibre in the small-angle beamline at ESRF (Dobbie *et al.*, 1998) with 20 μs time resolution. It may be the first triumph for the use of third-generation synchrotron radiation. Such an experiment points the way to other studies where interesting events take place.

8.1.3. *Two-dimensional time-resolved experiments*. It is clearly desirable to record two-dimensional data in all kinds of muscle diffraction experiments. The two-dimensional diffraction pattern has many reflections which are mutually related in origin. Therefore, it is meaningful and necessary to compare time courses of their intensity changes. Since we cannot expect all muscle preparations to

behave in exactly the same manner, the time courses to be compared should be desirably from the same preparation. However, most of the time-resolved experiments on muscle have been performed using linear X-ray detectors. This was mainly because fast area detectors were not available. Even when an area detector was used, sometimes only a part of the diffraction pattern was recorded (Irving *et al.*, 1992; Bordas *et al.*, 1993). One reason for this was asymmetric beam size. In the second-generation storage rings the beam at the specimen or detector tends to be elongated horizontally. This is most serious when the beam cannot be cut down in size because high intensity is required. The small and symmetric beam size in the third-generation storage rings has solved this problem. Although desirable, two-dimensional time-resolved experiments have not been performed very often. One example is an experiment using a video CCD camera equipped with an X-ray image intensifier (Yagi *et al.*, 1995). In their experiments, several reflections were recorded in a single contraction of frog sartorius whole muscle. The muscle was either stretched or released during isometric tetanus so that the responses to the length changes can be compared directly in the same specimen. For quantitative comparison of intensities under different conditions, this sort of experiment will be essential.

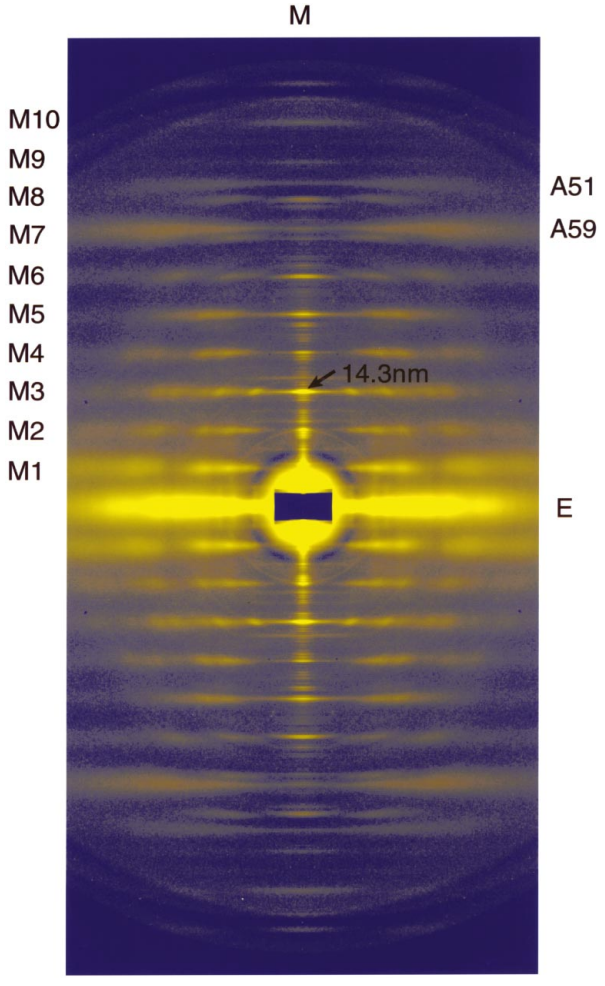

Figure 12
An example of an X-ray diffraction pattern from live frog muscle with a high spatial resolution. The pattern was taken using parallel beams from the undulator installed at the Tristan main ring at KEK. M and E are the meridional and equatorial axes. M1–M10 are the myosin-based reflections with a basic repeat of 42.9 nm. A51 and A59 are the 5.1 and 5.9 nm actin layer lines. Note the presence of numerous fine diffraction lines on the meridian, which come mainly from the interference between two halves of the thick filaments centred on the M-line in the sarcomere.

8.2. *Technical challenges*

From the above examples it is clear that there are two major challenges to the synchrotron radiation technology. One is high flux that is required to make high-time-resolution experiments possible. The other is a fast detector that can handle intense diffraction when this high flux is used.

8.2.1. *Obtaining higher flux.* To obtain a high flux with a small focus, a low-emittance storage ring is necessary. Several different approaches are envisaged to obtain high flux. (i) Place a bent monochromator close to the source (preferably a wiggler) to collect horizontal divergence as much as possible. Most of the small-angle diffraction beamlines in the second-generation storage rings used a horizontally bent monochromator for focusing. Since the horizontal acceptance is increased when the monochromator is closer to the source, this can be an efficient way to increase flux. Typical examples are the Daresbury 16.1 (Towns-Andrews *et al.*, 1989) and CHESS F1 (Irving & Huxley, 1994) beamlines. However, since the third-generation storage rings are larger than the second-generation rings, the distance from the source to the first optical element has to be larger, making it difficult to employ this design. (ii) Use a multilayer monochromator which has a wider bandwidth than an Si monochromator to increase the flux. A commonly used Si monochromator has a bandwidth of ~0.01%. In most muscle diffraction experiments this is unnecessarily small. A multilayer monochromator has a bandwidth of 1–3%. Although it is difficult to resolve closely spaced reflections (such as the two components of 14.5 nm myosin meridional reflections or the 44.1 nm C-protein meridional and the 38.5 nm troponin meridional reflections), most of the interesting reflections can be resolved with this bandwidth. A small-angle beamline in SSRL employed this design and achieved a flux of one order of magnitude higher than that with an Si monochromator (Tsuruta *et al.*, 1998). (iii) Use of an unmonochromatized undulator beam. This design has been used in the 'Troika' beamline at ESRF for X-ray photon correlation spectroscopy (Abernathy *et al.*, 1998) and the 'high flux' beamline at SPring-8. Focusing can be performed with mirrors which eliminate higher undulator harmonics. The bandwidth is 1–2%. The flux is 100–1000 times higher than that available in the beamlines of the second-generation rings. Although application of this type of beamline for diffraction studies has not been examined extensively as yet, this may be a highly useful design when the requirement is primarily high flux.

8.2.2. *Faster detectors*. It is becoming more and more difficult to cope with the flux. The classical photon-counting gas detector usually cannot handle more than 10^6 photons s^{-1}. Recent development pushed up this number to above 10^7 photons s^{-1} (RAPID by Daresbury Laboratory; Lewis, 1994) with a time resolution of 20 μs or better with the help of micro-gap technology and advanced electronics. However, photons in diffraction from a whole muscle are already close to this number even in currently available beamlines. Even when a single fibre is used as a specimen, the detector will not be fast enough if the flux is increased by using the designs described above.

Integrating-type detectors such as an image plate or a CCD can handle much higher intensity. However, their slow readout limits the time resolution. When an image plate is used as a streak camera, it can reach a time resolution of 23 μs (see Amemiya, 1995). When an X-ray image intensifier is coupled with a conventional video CCD for readout, 30 s^{-1} is the typical frame rate. Since the video camera is used in a 2:1-interlaced field-accumulation mode, one can obtain information from 60 individual frames per second. This system has been used at the Photon Factory in several muscle experiments (Yagi *et al.*, 1995, 1998) as mentioned above. When a digital CCD is used for readout, by reducing the number of scanning lines, a frame rate can be above 1000 s^{-1}. The disadvantage of integrating-type detectors, especially CCDs, is the readout noise. When an experiment is repeated and the images are added, noise is also added. Thus the image does not improve as much as in the case of the photon-counting detector which has no noise.

An ultimate detector would be a two-dimensional array of independent counters with a separate readout circuit and counter. One such example is a pixel array detector which is an array of Si solid-state detectors. A design for time-resolved experiments has already been tested at CHESS (Eikenberry *et al.*, 1998). However, it will take still more years to make a detector that has an area larger enough for muscle diffraction experiments. At the moment, the best practical compromise is to attenuate the strong part of the diffraction pattern, such as the equator, to avoid saturation of the detector and make the measurement of the weaker parts possible. A more sophisticated area detector with a high time resolution will open up the possibility of producing a three-dimensional cinema of the process of muscle contraction.

8.3. *Radiation damage: pessimistic versus optimistic*

Radiation damage is another important issue to overcome in future muscle experiments. A live muscle is usually damaged in a few seconds exposure at currently available beamlines. The damage seems to be a result of a break in the cell membrane because skinned fibres are more resistant to radiation than intact fibres. The damage can be avoided by moving the muscle during exposure to spread out the radiation over the muscle. However, when one is working with a single muscle fibre, this technique is not useful because the fibre is usually smaller than the beam. Although this appears to be a tragic situation, we should not be too pessimistic. The number of photons required to record one diffraction pattern with a certain quality is the same whether it is recorded in a 1 d exposure or a 1 ms exposure. Since the radiation damage mainly depends on the number of photons which are absorbed by the specimen, this means that we can still record a diffraction pattern with a high flux. What should be avoided is a quick rise in temperature which may happen when an extremely intense beam is used. The situation is certainly worse if a time course of an intensity change of a reflection has to be measured. In this case, as one is trying to record many successive diffraction patterns, the number of photons hitting the specimen has to be larger. However, even in this case, if the experiment can be performed at a 1 s time resolution without radiation damage, it can be performed at 0.1 ms time resolution with a beam that is 10000 times more intense as long as the number of frames is the same. Thus the high time resolution using a high flux is not serious. However, if one is trying to work at a higher time resolution for a longer period of time, the radiation damage becomes more serious. In most cases, one does not have to record a whole process at a high time resolution. For instance, force recovery after a quick length change has three components with a time constant of ~1, 3 and 20 ms. Thus, one does not need to record the slower process at a very high time resolution. It is desirable to reduce intensity and use a longer time frame for a slower phase. For this purpose it is necessary to develop a technique to control the intensity of the beam at one's will.

9. Conclusions

Although atomic structures of the myosin head and actin have been known for some years and that of troponin-bound tropomyosin will be elucidated soon, it still seems necessary to study muscle structures to understand the molecular mechanism of muscle contraction. Although one can postulate models of atomic interaction between myosin and actin, they are based upon static atomic structures of crystallized molecules. It requires good imagination to postulate interaction, and one has to realise that sometimes the reality is beyond imagination. For solid basis for a molecular model of contraction, X-ray fibre diffraction on intact muscle is still an important method because it tells us the dynamic molecular structure, albeit not atomic, of contracting muscle. Since the structural change is rapid, studies at a high time resolution using synchrotron radiation are indispensable. It will also be necessary to combine the molecular changes observed in muscle studies and a model of interaction based upon atomic structures. To understand the dynamic function of proteins and the protein–protein interaction in a cell at an atomic level is an ultimate goal in structural biology. Muscle research has been its best example, and it will continue to be. Muscle experiments are becoming more and more challenging.

The authors wish to thank their old and new colleagues for kind collaboration, particularly Dr Y. Amemiya for his continuous interest and encouragement. One of the authors (KW) thanks his collaborators Drs Y. Ueno, Y. Sugimoto and Y. Takezawa for their stimulative discussion and the use of unpublished data. Thanks are also due to Dr T. Arata for critical reading of the manuscript. They are grateful to Dr S. Hasnain, who has provided the opportunity to write this article on the occasion of the celebration issue of John Walker, and for valuable comments.

References

Abernathy, D. L., Grubel, G., Brauer, S., McNulty, I., Stephenson, G. B., Mochire, S. G. J., Sundy, A. R., Mulders, N. & Sutton, M. (1998). *J. Synchrotron Rad.* **5**, 37–47.

Amemiya, Y. (1995). *J. Synchrotron Rad.* **2**, 13–21.

Amemiya, Y., Satow, Y., Matsushita, T., Chikawa, J., Wakabayashi, K. & Miyahara, J. (1988). *Topic. Curr. Chem.* **147**, 121–144.

Amemiya, Y., Wakabayashi, K., Tanaka, H., Ueno, Y. & Miyahara, J. (1987). *Science*, **237**, 164–168.

Bordas, J., Diakun, G. P., Diaz, G., Harries, J. E., Lewis, R. A., Lowy, J., Mant, G., Martin-Fernandez, M. L. & Towns-Andrews, E. (1993). *J. Muscle. Res. Cell Motil.* **14**, 311–324.

Dobbie, I., Linari, M., Piazzesi, G., Reconditi, M., Koubassova, N., Ferenczi, M. A., Lombardi, V. & Irving, M. (1998). *Nature (London)*, **396**, 383–387.

Eikenberry, E. F., Barna, S. L., Tate, M. W., Rossi, G., Wixted, R. L., Sellin, P. J. & Gruner, S. M. (1998). *J. Synchrotron Rad.* **5**, 252–255.

Goldman, Y. E. & Huxley, A. F. (1994). *Biophys. J.* **67**, 2131–2136.

Griffith, P. J., Ashley, C. C., Bagni, M. A., Maeda, Y. & Cecchi, G. (1993). *Biophys. J.* **64**, 1150–1160.

Higo, J., Sugimoto, Y., Wakabayashi, K. & Nakamura, H. (1999). *J. Mol. Biol.* Submitted.

Holmes, K. C., Ropp, D. & Kabsch, G. W. (1990). *Nature (London)*, **347**, 44–49.

Holmes, K. C. (1997). *Curr. Biol.* **7**, R112–118.

Holmes, K. C. & Rosenbaum, G. (1998). *J. Synchrotron Rad.* **5**, 147–153.

Huxley, A. F. & Niedergerke, R. (1954). *Nature (London)*, **173**, 171–173.

Huxley, A. F. & Simmons, R. M. (1971). *Nature (London)*, **233**, 533–538.

Huxley, H. E. (1969). *Science*, **164**, 1356–1366.

Huxley, H. E. (1973). *Cold Spring Harbor Symp. Quant. Biol.* **37**, 361–376.

Huxley, H. E. & Brown, W. (1967). *J. Mol. Biol.* **30**, 383–434.

Huxley, H. E. & Hanson, J. (1954). *Nature (London)*, **173**, 973–974.

Huxley, H. E. & Holmes, K. C. (1997). *J. Synchrotron Rad.* **4**, 366–379.

Huxley, H. E., Stewart, A. & Irving, T. C. (1998). *Adv. Exp. Med. Biol.* **453**, 281–288.

Huxley, H. E., Stewart, A., Sosa, H. & Irving, T. C. (1994). *Biophys. J.* **67**, 2411–2421.

Irving, M., Lombardi, V., Piazzesi, G. & Ferenczi, M. A. (1992). *Nature (London)*, **357**, 156–158.

Irving, T. C. & Huxley, H. E. (1994). *Synchrotron Radiation in the Biosciences*, edited by B. Chance, J. Deisenhofer, S. Ebashi, D. T. Goodhead, J. R. Helliwell, H. E. Huxley, T. Iizuka, J. Kirz, T. Mitsui, E. Rubenstein, N. Sakabe, T. Sasaki, G. Schmahl, H. B. Stuhrmann, K. Wüthrid & G. Zaccai, pp. 517–529. Oxford: Clarendon Press.

Kabsch, W., Mannherz, H. G., Suck, D., Pai, E. F. & Holmes, K. C. (1990). *Nature (London)*, **347**, 37–44.

Kato, H., Miyahara, J. & Takano, M. (1985). *Neurosurg. Rev.* **8**, 53–57.

Lenart, T. D., Murray, J. M., Franzini-Armstrong, C. & Goldman, Y. E. (1996). *Biophys. J.* **71**, 2289–2306.

Lewis, R. (1994). *J. Synchrotron Rad.* **1**, 43–53.

Maeda, Y., Popp, D. & McLaughlin, S. M. (1988). *Adv. Exp. Med. Biol.* **226**, 381–390.

Phillips, G. N. Jr, Fillers, J. P. & Cohen, C. (1986). *J. Mol. Biol.* **192**, 111–131.

Piazzesi, G. & Lombardi, V. (1995). *Biophys. J.* **68**, 1966–1979.

Piazzesi, G., Reconditi, M., Dobbie, I., Linari, M., Boesecke, P., Diat, O., Irving, M. & Lombardi, V. (1999). *J. Physiol.* **514**(2), 305–312.

Podolsky, R. J., Onge, R. St., Yu, L. & Lymn, R. W. (1976). *Proc. Natl Acad. Sci. USA*, **73**, 813–817.

Rayment, I., Rypniewski, W. R., Schmidt-Base, K., Smith, R., Tomchick, D. R., Benning, M. M., Winkelmann, D. A., Wasenberg, G. & Holden, H. M. (1993). *Science*, **261**, 50–58.

Reedy, M. K. (1993). *Structure*, **1**, 1–5.

Squire, J. M. & Morris, E. P. (1998). *FASEB J.* **12**, 761–771.

Sugimoto, Y., Tokunaga, M., Takezawa, Y., Ikebe, M. & Wakabayashi, K. (1995). *Biophys. J.* **68**, 29–34.

Sugimoto, Y., Tokunaga, M. & Wakabayashi, K. (1999). In preparation.

Takezawa, Y., Sugimoto, Y., Kobayashi, T. & Wakabayashi, K. (1998). *Adv. Exp. Med. Biol.* **453**, 309–317.

Takezawa, Y., Sugimoto, Y., Kobayashi, T. & Wakabayashi, K. (1999). In preparation.

Towns-Andrews, E., Berry, A., Bordas, J., Mant, G. R., Murray, P. K., Roberts, K., Sumner, I. L., Worgan, J. S., Lewis, R. A. & Gabriel, A. (1989). *Rev. Sci. Instrum.* **60**, 2346–2349.

Tsuruta, H., Brennan, S., Rek, S. U., Irving, T. C., Tompkins, W. H. & Hodgson, K. O. (1998). *J. Appl. Phys.* **31**, 672–682.

Ueno, Y., Moriwaki, N. & Wakabayashi, K. (1994). *Synchrotron Radiation in the Biosciences*, edited by B. Chance, J. Deisenhofer, S. Ebashi, D. T. Goodhead, J. R. Helliwell, H. E. Huxley, T. Iizuka, J. Kirz, T. Mitsui, E. Rubenstein, N. Sakabe, T. Sasaki, G. Schmahl, H. B. Stuhrmann, K. Wüthrid & G. Zaccai, pp. 441–450. Oxford: Clarendon Press.

Ueno, Y., Takezawa, Y. & Wakabayashi, K. (1999). In preparation.

Vassylyev, D. G., Takeda, S., Wakatsuki, S., Maeda, K. & Maeda, Y. (1998). *Proc. Natl Acad. Sci. USA*, **95**, 4847–4852.

Wakabayashi, K. & Amemiya, Y. (1991). *Handbook Synchrotron Rad.* **4**, 597–678.

Wakabayashi, K., Saito, H., Moriwaki, N., Kobayashi, T. & Tanaka, H. (1993). *Adv. Exp. Med. Biol.* **332**, 451–460.

Wakabayashi, K., Sugimoto, Y., Tanaka, H., Ueno, Y., Takezawa, Y. & Amemiya, Y. (1994). *Biophys. J.* **67**, 2422–2435.

Wakabayashi, K., Sugiyama, H., Yagi, N., Irving, T. C., Iwamoto, H., Horiuti, K., Takezawa, Y., Sugimoto, Y., Ogino, M., Iino, S., Kim, D.-S., Majima, T., Amemiya, Y., Yamamoto, S. & Ando, M. (1998). *J. Synchrotron Rad.* **5**, 280–285.

Wakabayashi, K., Tokunaga, M., Kohno, I., Sugimoto, Y., Hamanaka, T., Takezawa, Y., Wakabayashi, T. & Amemiya, Y. (1992). *Science*, **258**, 443–447.

Yagi, N., Amemiya, Y. & Wakabayashi, K. (1995). *Jpn. J. Physiol.* **45**, 583–606.

Yagi, N., Horiuti, K. & Takemori, S. (1998). *J. Muscle Res. Cell Motil.* **19**, 75–86.

Yagi, N. & Takemori, S. (1995). *J. Muscle Res. Cell Motil.* **16**, 57–63.

Yagi, N., Takemori, S. & Watanabe, M. (1993). *J. Mol. Biol.* **231**, 668–677.

Yagi, N., Wakabayashi, K., Iwamoto, H., Horiuti, K., Kojima, I., Irving, T. C., Takezawa, Y., Sugimoto, Y., Iwamoto, S., Majima, T., Amemiya, Y. & Ando, M. (1996). *J. Synchrotron Rad.* **3**, 305–312.